J. Meas. Sci. Instrum., 2024, 15(3): 344-359. http://jmsi.publish.founderss.cn
DOI: 10.62756/jmsi.1674-8042.2024036 jmsi@nuc.edu.cn

Improved AVOA based on LSSVM for wind power prediction

ZHANG Zhonglin[1*], WEI Fan[1], YAN Guanghui[1], MA Haiyun[2]

1. School of Electronic and Information Engineering, Lanzhou Jiaotong University, Lanzhou 730070, China;
2. School of Mechanical and Informational Science, Tianshui Normal University, Tianshui 741001, China

***Corresponding author:** ZHANG Zhonglin (zhangzl@mail.lztju.cn)

Received: March 8, 2023 **Revised:** May 10, 2023 **Accepted:** May 17, 2023

Abstract: Improving the prediction accuracy of wind power is an effective means to reduce the impact of wind power on power grid. Therefore, we proposed an improved African vulture optimization algorithm (AVOA) to realize the prediction model of multi-objective optimization least squares support vector machine (LSSVM). Firstly, the original wind power time series was decomposed into a certain number of intrinsic modal components (IMFs) using variational modal decomposition (VMD). Secondly, random numbers in population initialization were replaced by Tent chaotic mapping, multi-objective LSSVM optimization was introduced by AVOA improved by elitist non-dominated sorting and crowding operator, and then each component was predicted. Finally, Tent multi-objective AVOA-LSSVM (TMOALSSVM) method was used to sum each component to obtain the final prediction result. The simulation results show that the improved AVOA based on Tent chaotic mapping, the improved non-dominated sorting algorithm with elite strategy, and the improved crowding operator are the optimal models for single-objective and multi-objective prediction. Among them, TMOALSSVM model has the smallest average error of stroke power values in four seasons, which are 0.069 4, 0.054 5 and 0.021 1, respectively. The average value of DS statistics in the four seasons is 0.990 2, and the statistical value is the largest. The proposed model effectively predicts four seasons of wind power values on lateral and longitudinal precision, and faster and more accurately finds the optimal solution on the current solution space sets, which proves that the method has a certain scientific significance in the development of wind power prediction technology.

Key words: African vulture optimization algorithm (AVOA); least squares support vector machine (LSSVM); variational mode decomposition (VMD); multi-objective prediction; wind power

0 Introduction

In recent years, global warming, serious air pollution and other ecological environmental damage have forced carbon reduction and renewable energy utilization accelerated[1]. To this end, China strongly supports the development of distributed wind power and photovoltaic power, and encourages local governments to use wind power in areas with water shortage, fuel shortage and inconvenient transportation, so as to realize the sustainable development of new energy[2]. However, wind power is an unstable energy with random fluctuations, and large-scale integration of wind power into the system will certainly bring new challenges to the stability of power supply system. Therefore, wind power prediction has gradually become a key basic technology in the field of wind power generation.

The research methods of wind power prediction can be roughly divided into three categories: physical model, statistical model, and machine learning[3]. To characterize the uncertainty and dependent structure of wind turbine output in wind farm, Ye et al.[4] proposed a short-term wind power prediction method based on physical method and spatial correlation. However, the method is insufficient in realizing high-precision data acquisition and real-time fast transmission. The statistical method[5] is a mathematical model based on historical data to predict wind speed and force, but its modeling premise is to keep wind speed in a linear normal distribution. Zhang et al. [6] established autoregressive integrated moving average model (ARIMA) to predict the time series of actual output power with five time resolutions, but this model has not fully considered the characteristics of wind power distribution, time correlation and time distribution, and so on, so many scholars believe that the method is not suitable for wind power prediction. At present, machine learning has been studied extensively and in depth owing to its excellent nonlinear fitting ability[7], such as back propagation (BP) [8] and radial basis function (RBF) [9]. However, traditional

machine learning algorithms have certain disadvantages in solving high-dimensional nonlinear sequence problems, and are susceptible to the coupling degree and robustness of different variables, thus limiting their application scope. By comparison, the least squares support vector machine (LSSVM) [10] can project nonlinear input variables into high-dimensional space to construct optimal decision surface, thus reducing the computational complexity and speeding up the processing speed of nonlinear and high-dimensional pattern recognition problems, which is suitable for predicting the time series sample data of wind power with strong volatility.

Variational mode decomposition (VMD) is a time-frequency signal decomposition method[11], which treats the original time series as a group of unstable signals for processing and analysis. Aiming at the non-stationary and nonlinear characteristics of wind power, Zhao et al.[12] used VMD to decompose the upper and lower limits of wind power into several sub-components, and then added up the prediction results of these sub- components to obtain the final prediction result, thus improving the multi-step interval prediction accuracy of ultra-short-term wind power. Wang et al. [13] used VMD to decompose the historical power data into trend component, detail component and random component to reduce the complexity and instability of the original power data, optimized the parameters of LSSVM with the improved bat algorithm (IBA), predicted each sub-mode respectively, and superimposed the prediction results of sub-modes to obtain the final power generation prediction result. Since the prediction accuracy of LSSVM is easily affected by penalty parameters and kernel parameters, some scholars use swarm intelligence optimization algorithm to optimize its parameters so as to improve the prediction accuracy. Wei et al.[14] proposed sparrow search algorithm (SSA) to optimize the parameters of LSSVM model, which solves the problem of low efficiency of parameter optimization of LSSVM. However, the problems that the algorithm is easy to fall into local optimum and lacks population diversity in the late iteration are not considered. Cheng et al. [15] improved the "teaching" and "learning" stages of the basic teaching-learning-based optimization (TLBO) algorithm by introducing adaptive factors and Gaussian mutation operator to improve the global search and convergence of the algorithm. Tong et al.[16] introduced logistic chaotic mapping and adaptive weight into the SSA to improve the uniformity of population distribution and the search ability of the algorithm, which is used to optimize the key parameters of LSSVM. However, logistic mapping has the problem of fixed point, that is, after many iterations, it tends to be a fixed value, which reduces the search efficiency and ability of the algorithm. Compared with logistic mapping, the chaos sequence generated by Tent mapping proposed later overcomes the shortcoming of traditional optimization algorithm that it is easy to fall into local optimal solution, which can realize fast optimization and speed up the chaos iteration speed generated in the interval of [0, 1]. Huang[17] used the uniformity and ergodicity of Tent chaotic mapping to generate the location information of initial sparrow population, which increases the diversity of sparrow population and improves the convergence speed and global search ability of SSA. In fact, not only the coordinated control of wind storage, but also many optimal controls of power system need to solve the multi-objective optimization problem. For example, Liu et al.[18] considered the problem of wind and light abandoning in the Three North regions, made full use of "source-charge" resources at different time scales, and proposed a multi-time and multi-scale power system coordination scheduling optimization strategy. Yu et al.[19] proposed a multi-objective prediction method of short-term load of microgrid considering probability interval, so as to effectively improve the accuracy and reliability of short-term load interval prediction of microgrid. However, the objective function of the above-mentioned multi-objective optimization model considers only prediction accuracy and stability of the prediction model, and does not involve the prediction accuracy of wind power in data direction. Therefore, considering the power generation characteristics of cut-in wind speed and cut-out wind speed to reduce the dead zone range in the wind vane and improve the direction prediction accuracy can ensure the mechanical reliability of the anemometer.

On the whole, the existing wind power prediction models are not perfectly establised because there are some errors in their input sequences, stochastic volatility of the wind is less considered, optimization algorithms easily fall into local optimal solutions, or most of wind power prediction cannot balance the stability and the accuracy of wind power prediction. In this study, we analyzed the effects of two froms of fan bearing clearance on the length of component service cycle and the utilization rate of resources, and proposed a new multi-objective hybrid prediction model for wind power optimization by taking transverse and longitudinal prediction accuracy as objective functions, VMD as denoising reconstruction method, and Tent chaotic mapping as an improved optimization algorithm. After the original sequence was effectively decomposed into a series of relatively stable eigenmode

components, the improved multi-objective optimization algorithm was used to predict each component. Finally, the proposed hybrid model was used to integrate and add up the prediction results of all components as the final prediction result. Experimental results show that Tent chaotic mapping multi-objective African vulture optimization algorithm (AVOA) [20] LSSVM (TMOALSSVM) algorithm has better optimization performance and stability than other models.

1 Related work

1.1 Relevant algorithm

Metaheuristic algorithms play an important role in solving optimization problems. Most of these algorithms are inspired by collective intelligence and foraging in nature. In this study, a new metaheuristic algorithm was proposed, which was inspired by African condor lifestyle, and called AVOA. It simulated the foraging and navigation behaviors of African vultures.

1.2 VMD

VMD can effectively process nonlinear and non-stationary signals. In the process of acquiring decomposed components, the frequency center and bandwidth of each component are determined by iteratively searching the optimal solution of the variational model, so that the frequency domain subdivision of signals and effective separation of each component can be realized adaptively. Its overall framework is variational problem, with each mode obtaining the mininum sum of estimated bandwidths and being limited with different central frequency bandwidths. To solve this problem, the alternating direction multiplier method is used to update the mode and its central frequency. Then, each mode is gradually demodulated to the corresponding base band, Finally, the corresponding central frequencies of all modes are extracted together. The goal of VMD is to decompose the real input signal into a discrete number of sub-signals that have a specific sparsity when reproducing the input signal. Sparsity is reflected in the bandwidth of the spectral domain. In other words, each sub-signal is assumed to revolve mainly around the central frequency, which will be determined by decomposition.

1.3 LSSVM

LSSVM is a combination of support vector machine (SVM) and least squares (LS) mathematical optimization technology, LS minimizes the sum of squared errors between the predict value and the actual value to find the best function match of the predict value. To solve the nonlinear fitting problem, the kernel function is used to map the sample into a higher dimensional space, and the regression problem is transformed into an optimization problem with equality constraints. It is expressed as

$$\min J(\boldsymbol{W},\varepsilon)=\frac{1}{2}\|\boldsymbol{W}\|^2+c\sum_{i=1}^{N}\varepsilon_i^2,$$
$$\text{s.t. } y_i=\left\langle \boldsymbol{W}^{\mathrm{T}},\varphi(x_i)\right\rangle+b+\varepsilon_i,\ i=1,2,\cdots,N, \quad (1)$$

where $\boldsymbol{W}$ is the weight matrix, $\varphi(\cdot)$ is the nonlinear function; c is the penalty factor; and ε_i is the fitting error of the ith sample.

Introducing Lagrange multiplier $\alpha>0$, the above optimization problem is converted into unconstrained optimization problem. It is defined as

$$L=\frac{1}{2}\|\boldsymbol{W}\|^2+\frac{1}{2}\gamma\sum_{i=1}^{N}\varepsilon_i^2-$$
$$\sum_{i=1}^{N}\alpha_i\left\{\left\langle \boldsymbol{W}^{\mathrm{T}},\varphi(x_i)\right\rangle+b+\varepsilon_i-y_i\right\}, \quad (2)$$

where γ is a regularization parameter balancing complexity and precision of the model, and ε_i is the error value.

LSSVM transforms the optimization process into linear equation solution, which reduces the difficulty of solution. The Gaussian kernel is selected as the kernel function for high-dimensional mapping. Finally, the mathematical model of LSSVM can be expressed as

$$y(x)=\sum_{i=1}^{N}\alpha_i K(x_i,x_j)+b. \quad (3)$$

As we know, the choice of kernel function will directly affect the performance of the model, where $K(x_i,x_j)=\exp\left[-\left(x_i-x_j\right)^2/\left(2\delta^2\right)\right]$ is a Gaussian kernel function, and δ is the width of kernel function.

2 TMOAVOA

To apply AVOA to multi-objective optimization problems, we draw lessons from the idea of nondominated sorting genetic algorithm with elite strategy in multi-objective evolutionary algorithm (MOEA), and introduce nondominated hierarchical method as well as congestion and fitness sharing strategy into AVOA algorithm, so as to help good vulture individuals have a greater chance to inherit the next generation. As a result, the noninferior solution individuals are evenly distributed, the diversity of vulture population is maintained, the over reproduction of super individuals is overcome, and the premature

convergence of the algorithm is prevented. Furthermore, the random number in population initialization is replaced by Tent chaotic maping, so that the random factor can traverse the whole interval, increase the diversity of vulture population, and improve the global search ability of the algorithm.

2.1 AVOA

AVOA was proposed by Benyamin et al. in 2021, and inspired by the foraging and navigation behaviors of African vultures. It has high speed and high solving accuracy, and is widely used in single-objective optimization.

2.1.1 Optimal vultures

After the initial population is formed, the fitness values of all solutions are calculated. The best solution is selected as the best condor in the first group, and the suboptimal solution is selected as the best condor in the second group. For each fitness iteration, the entire population is recalculated. The best solutions for the first set and the second set are defined as

$$R(i)=\begin{cases} V_1, & p(i)=L_1, \\ V_2, & p(i)=L_2, \end{cases} \tag{4}$$

where $p(i)$ respresents the probability that the vulture is selected to move other vultures to be one of the best individuals in each group; L_1 and L_2 are the parameters given before the search operation, their values are within [0, 1], and the sum of these two parameters is 1. The probability of the optimal solution is defined as

$$p(i)=\frac{F_i}{\sum_{i=1}^{n}F_i}. \tag{5}$$

It obtains the probability of selecting the best solution, at which the best solution for each group is selected.

2.1.2 Satiety rate

Inspired by the speed at which vultures feed or starve, the algorithm moves the exploration phase to the development phase. This stage can be described as

$$t=h\left[\sin\left(\frac{\pi}{2}\frac{i}{M_i}\right)+\cos\left(\frac{\pi}{2}\frac{i}{M_i}\right)-1\right], \tag{6}$$

where i represents the current number of iterations, M_i represents the maximum number of iterations, and h is a random number within $[-2,2]$.

Satiety rate shows a downward trend, and this behavior can be represented by

$$F=(2r_1+1)z\left(1-\frac{i}{M_i}\right)+t, \tag{7}$$

where F indicates that the vulture is full, z is a random number within $[-1,1]$ and changes after every iteration, and r_1 is a random number within $[0,1]$.

2.1.3 Exploration phase

In AVOA, vultures can examine different random areas based on two different strategies, and use a parameter called p_1 to select either strategy. This parameter must be assigned before the search operation, and its value should be within $[0,1]$.

$$p(i+1)=\begin{cases} E(9), & p_1\geqslant r_1, \\ E(11), & p_1<r_1. \end{cases} \tag{8}$$

To determine which strategy to be adopted in the exploration phase, a random number within $[0,1]$ need to be generated. In this way, each vulture randomly searches the areas that make it feel full. It can be expressed as

$$p(i+1)=R(i)-D(i)F, \tag{9}$$

where $R(i)$ is one of the best vultures and selected in the current iteration.

The calculation process of $D(i)$ can be expressed as

$$D(i)=\left|XR(i)-p(i)\right|, \tag{10}$$

where X is the position in which vultures move randomly to protect food from other vultures. X is used to increase the coefficient vector of random motion, which will change with each iteration and is obtained by $X=2r$, where r is the random number within $[0,1]$.

The current vector position of the vulture is defined as

$$p(i+1)=R(i)-F+r_2\left[(u-l)r_3+l\right], \tag{11}$$

where u and l are the upper and lower limits for optimization, respectively; r_2 and r_3 are random numbers within $[0,1]$.

2.1.4 Development phase

When the satiety rate F is within [0.5, 1], the algorithm enters the first stage of development phase, in which two different rotational flight and siege strategies are executed. The location is update by

$$p(i+1)=\begin{cases} E(13), & p_2\geqslant r_{p2}, \\ E(16), & p_2<r_{p2}, \end{cases} \tag{12}$$

where p_2 is the probability to choose the strategy, and it must be assigned a value within [0, 1] before the search operation is performed. At the beginning of this phase, r_{p2} is generated, which is a random number within $[0,1]$. If the value r_{p2} is greater than or equal to the parameter p_2, the siege strategy is implemented slowly.

Vultures are relatively energetic when the satiety reate F is greater than 0.5. The movement formula is

$$d(y)=R(i)-p(i), \tag{13}$$

where $d(y)$ represents the distance between the vulture and the best vulture of the two groups.

However, if the random number is less than the parameter, the rotation flight strategy is executed. Vultures often make whirling flights to simulate spiral motion. The spiral model has been used in the mathematical modeling of rotary flight. In this method, a spiral equation is established between all vultures and one of the two best vultures, namely

$$p(i+1)=R(i)-\left\{\left[R(i)\frac{r_5 p_i}{2\pi}\cos(p(i))\right]+\left[R(i)\frac{r_5 p_i}{2\pi}\sin(p(i))\right]\right\}, \tag{14}$$

where r_5 is a random number between 0 and 1.

When the satiety rate is less than 0.5, the leader vultures become hungry and weak, and do not have enough energy to fight the other vultures, whereas other vultures become aggressive in their search for food. They move in different directions, and the movement can be expressed as

$$p(i+1)=\frac{A_1+A_2}{2}, \tag{15}$$

where A_1 and A_2 are the best vultures in the first group and in the second group, respectively. Furthermore, we have

$$p(i+1)=R(i)-|d(t)|FLevy(d), \tag{16}$$

where $d(t)$ represents the distance between the vulture and the best vulture in the two groups, and $Levy(d)$ represents the Levy flight mechanism.

Levy flight mechanism is expressed as

$$Levy(d)=0.01\frac{u\sigma\left(\dfrac{\Gamma(1+\beta)\sin\left(\dfrac{\pi\beta}{2}\right)}{\Gamma\left(\dfrac{1+\beta}{2}\right)\beta 2^{\frac{\beta-1}{2}}}\right)^{\frac{1}{\beta}}}{|v|^{\frac{1}{\beta}}}, \tag{17}$$

where β is the fixed default value 1.5; u and v all obey normal distribution, $u\sim N(0,\sigma^2)$, and $v\sim N(0,1)$

2.2 TAVOA

To improve the ability of global search and jump out of local optimum, some scholars put forward the idea of using chaotic sequence to make random factors approach the optimal solution with a certain probability, so as to shorten the running time of the algorithm and ensure global convergence and population diversity. For logistic mapping fixed point problem, that is, after many iterations, the search efficiency and ability of the algorithm reduces to a fixed value, Tent mapping is produced by chaotic sequence, which overcomes the shortcoming of local optimum, achieves rapid optimization, and speeds up the iteration within [0, 1]. Therefore, Tent chaotic mapping is used to initialize the population in AVOA algorithm, which helps the population traverse the whole solution space and improves the performance of the algorithm at the exploration stage. Tent mapping function is defined as

$$x_{i+1}=\begin{cases}2x_i, & 0\leqslant x_i<1/2,\\ 2(1-x_i), & 1/2\leqslant x_i\leqslant 1,\end{cases} \tag{18}$$

where x_i is the value of chaotic sequence in Tent chaotic mapping in the interval of [0, 1].

However, due to the problem of byte length, as mentioned in Ref. [22], x_i will generate a fixed value after several iterations. For example, when $x_i\in\{0.2,0.4,0.6,0.8\}$ or $x_i\in\{0,0.25,0.5,0.75\}$, the Tent chaotic mapping falls into a non-randomly cyclic state. Here, algorithm1 gives the pseudo-code of population initialization of TAVOA algorithm, and it represents the random number in the interval of [0, 1].

Algorithm 1:TAVOA population initialization

1. $v_0\in$ Rand[0, 1];
2. **While** $v_0\in\{0.2,0.4,0.6,0.8\}$ **do**
3. Regenerate random number v_0;
4. **end While**
5. **For** vulture i from 1 to N **do**
6. $v_i=\text{Tent}(v_{i-1})\begin{cases}2v_{i-1}, & 0\leqslant v_{i-1}<0.5\\ 2(1-v_{i-1}), & 0.5\leqslant v_{i-1}\leqslant 1\end{cases}$
7. **While** $v_0\in\{0,0.25,0.5,0.75\}$ **do**
8. $v_i=v_i+\mathbf{C}$;
9. **end While**
10. $X_i^0=v_i(u-l)+l$;
11. **end For**

2.3 Nondominant order of condor individuals

Since the fitness value of multi-objective AVOA (MOAVOA) is not a single function value, it cannot be calculated in the form of unique solution of the function. Therefore, in the multi-objective algorithm, the condor population need to be sorted in a non-dominant order to determine the fitness value, and the suitable individuals are selected to form the new parent population and offspring population according to the nondominant relationship and the crowding degree of individuals.

Assuming that the condor population is Q, two parameters $N(Q)$ and $S(Q)$ of each individual Q in the population are calculated, where $N(Q)$ is the number of dominant individuals in the population, and $S(Q)$ is the number of dominated individuals in the population. Traversing the entire population, the total

computational complexity of the two parameters is $O(mN^2)$. The main steps of the nondominated sorting algorithm are as follows:

1) Finding all individuals in the population whose $N(q)$ value is 0 and saving them in the current set $F(1)$;

2) For each individual i in the current set $F(1)$, its dominant individual set is S_i. Traversing each individual one time in S_i, and executing $n_i = n_i - 1$; If $n_i = 0$, saving the individual in set H;

3) Taking the individual obtained in $F(1)$ as the individual of the first nondominated layer and H as the current set, and repeating the above operation until the whole population is graded.

2.4 External archiving

In multi-objective African vulture individual algorithm, vulture population need to be nondominatedly sorted to determine the fitness. Furthermove, an external archive is needed to store multiple global optimal locations and the historically optimal position individuals and update them, thus maintaining the diversity of population and the global search ability, and avoiding premature convergence. The external archiving steps of the MOAVOA are as follows:

1) During each iteration, the algorithm judges whether there is a solution in the current external archive that can dominate the new individual generated by the iteration. If yes, the new individual need not to join the external archive; Otherwise, the new individual will control the existing solution in the external archive and replace the solution that is dominated by it in the external archive.

2) If the new individuals generated in the iteration process do not match the existing individuals in the external archive, the new individuals are stored in the external archive.

3) In the iterative update process, the information stored in the external archive will gradually increase. If the number of individuals in the archive exceeds the upper limit of the external archive, the overflow phenomenon will occur, resulting in the algorithm falling into local optimum. To keep the number of condor populations in the external archive within the upper limit, crowding operator is introduced to represent the relationship between dominant and nondominant individuals and the degree of superiority and inferiority of individuals, so as to eliminate similar individuals in the archive and maintain the diversity of population. The crowding degree can be expressed as

$$d = \sum_{k=1}^{m} \frac{z_k(i+1) - z_k(i-1)}{z_k^{\max} - z_k^{\min}}. \tag{19}$$

Ranking all individuals in the population in ascending order according to each objective function. The crowding distance from the first indivdual to last individual is set to infinity, $z_k(i+1)$ and $z_k(i-1)$ are the sum of the difference values between the values of all objective functions of the $i+1$ and the $i-1$ individuals.

4) All the individuals in the archive have their own crowding attribute. If the number of individuals in the external archive exceeds the upper limit, the individuals with large crowding value should be retained and those with small crowding value should be eliminated to improve the uniformity of optimal solution distribution throughout the interval.

2.5 TMOAVOA

Combined with the algorithms and strategies proposed above, we proposed TMOAVOA. The flow chart of algorithm is shown in Fig.1.

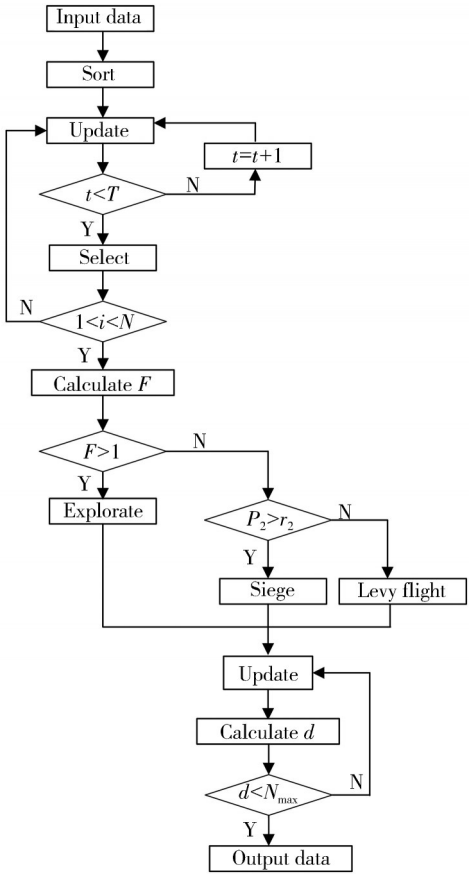

Fig. 1 Flow chart of TMOAVOA

Table 1 presents the specific parameter settings.

Table 1 TMOAVOA parameters

Parameter	Description
N	Vulture population
N_{max}	Maximum scale
T	Maximum iterations
L_1 and L_2	Random numbers (exploration phase)
p_1 and p_2	Random numbers (development phase)
k	Probability

3 TMOALSSVM model

Considering the power generation characteristics of cut-in and cut-out wind speeds, it is necessary to improve the mechanical reliability and direction prediction accuracy of the anemometer to reduce the dead zone range of the vane. The wind speed at a particular location varies as time goes by, and it may also be affected by the location of wind farms or the structure of turbines at other locations. Therefore, it is necessary to establish an appropriate prediction model in the region according to the characteristics of continuous wind speed change in space, correlation with the surrounding environment, and interaction of wind turbines, so as to predict the location at the next moment based on known location information and characteristics of wind power time series sample data. Due to the wind drift, wind power is usually unstable. To avoid relevant data being too simplex and unconvincing, direction accuracy objective function is chosen to calculate transverse and longitudinal prediction data of wind speed. Taking account of correlation information of prediction results in two directions instead of simplex single wind speed from wind farm, local wind power prediction accuracy can be improved. Therefore, to improve the prediction accuracy of wind speed, ensure the safety of wind power generation, and maintain the stability of the power system, we choose transverse prediction accuracy and longitudinal prediction accuracy as the objective functions of nonlinear wind power time series prediction. It can be defined as

$$F=\begin{cases}\min F_1(x)=\dfrac{1}{N}\left|y_i-y_i^*\right|,\\ \max F_2(x)=\dfrac{1}{N}\sum\limits_{i=1}^{N}\omega_i,\end{cases}\tag{20}$$

where y_i is the real wind power value at a certain moment, y_i^* is the predicted wind power value at a certain moment, and N is the original length of wind power time series. The constraint is $g(x)=(y_i-y_{i-1})(y_i^*-y_{i-1})>0$. When the constraint condition is met, ω_i is 1; otherwise, it is 0.

In this study, the classical multi-objective optimization strategy, weight coefficient method, is used to assign weight $O_i(x)(i=1,2)$ corresponding to each objective function $F_i(x)(i=1,2)$. By performing weighted linear combination of multiple optimization objective functions to minimize the sum of the two objective functions, the final optimization expression is

$$\min F=\sum_{i=1}^{m}O_iF_i(x),\ \text{s.t.}\sum_{i=1}^{m}O_i=1,O_i>0,\tag{21}$$

where m is the number of objective functions and O_i is the weight of each objective function.

To improve the prediction accuracy of non-stationary wind power time series, considering the influence of the two forms of gaps between fan bearings on the service life of components and resource utilization, as well as nonlinear time series of wind power, taking the transverse prediction accuracy and longitudinal. prediction accuracy as objective functions, a new hybrid model based on VMD, TMOAVOA and LSSVM for wind power prediction with multi-objective optimization is proposed. After the original sequence is effectively decomposed into a series of relatively stable eigenmode components, the improved multi-objective optimization algorithm is used to predict each component. Finally, this hybrid model integrates the prediction results of all components as the final prediction result. This combined TMOAVOA-VMD-LSSVM model contains the following steps:

1) VMD method is used to decompose the original wind power time series to reduce the complexity and non-stationarity of the original series.

2) In TMOAVOA algorithm, iteration times and population number are first initiallized. Then, it assigns certain weights to the two objective functions, which means horizontal accuracy and longitudinal accuracy are taken into account at the same time. Finally, the multi-objective problem is transformed into a single-objective optimization problem, and the objective function value is calculated.

3) TMOAVOA genetic algorithm is used again to optimize the penalty parameters and kernel parameters of LSSVM to improve the prediction accuracy of the model.

4) The optimized LSSVM model is used for finalwind power prediction.

The specific flow chart is shown in Fig.2

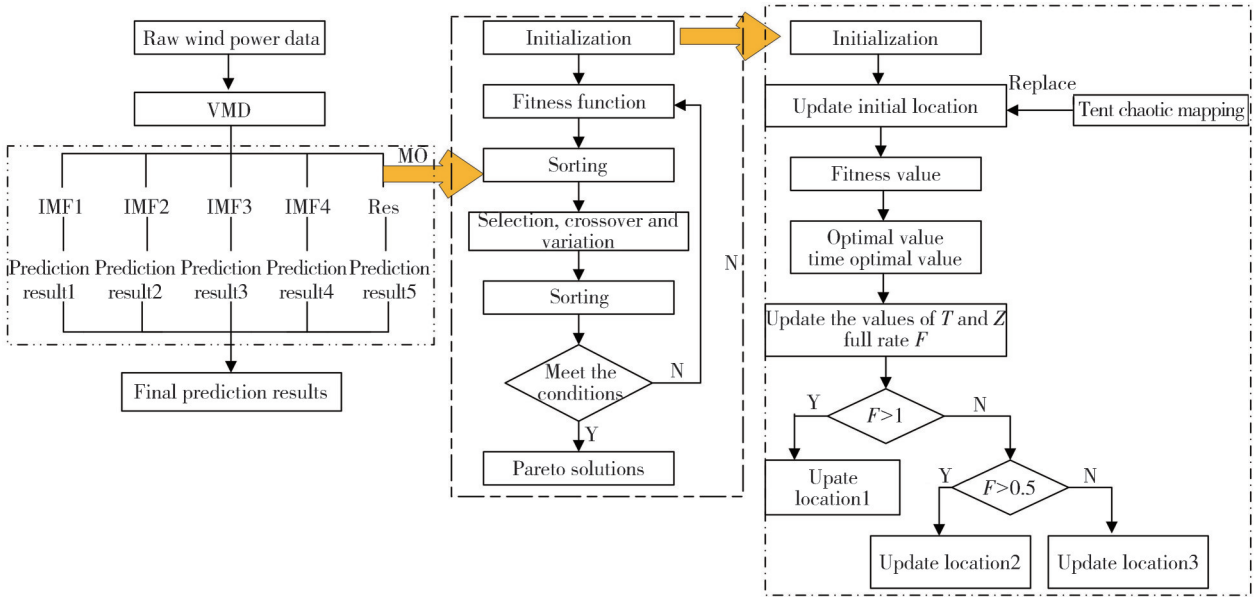

Fig. 2 Flow chart of hybrid TMOALSSVM model

4 Experiment

4.1 Comparison of algorithms

In this section, three groups of comparative experiments were designed. In the first group, four low-dimensional test functions were selected for testing. In the second group, four high-dimensional single-objective test functions were selected for testing. In the third group, four high-dimensional multi-objective test functions were selected to test. In the single objective experiment, the AVOA, TAVOA[21], Chameleon group optimization algorithm (CSA)[22], Sparrow search algorithm (SSA), Tent chaotic map Sparrow search algorithm (TSSA)[17], Logistic mapping sparrow search algorithm (LOGISTIC), and teaching and learning algorithm (TLBO) were compared, and the algorithm performance was evaluated by the convergence speed and accuracy of the algorithm. In the multi-objective experiment, the multi-objective sparrow search optimization algorithm (MOSSA), multi-objective optimization Chameleon algorithm using non-dominated sorting (MNCSA)[23], and MOAVOA were compared in the average running time, and the convergence speed and distribution of the solution sets were intuitively demonstrated by the non-inferior solution fitting diagram of the algorithm on each test problem.

4.1.1 Low-dimensional single objective functions

To verify the performance of the improved African condor algorithm using Tent chaotic mapping on low-dimensional test functions, four low-dimensional test functions were selected for experiment. The specific expression, dimension, initial search space and optimal solution of the objective function of the four low-dimensional test functions are shown in Table 2.

Table 2 Low dimensional single objective functions

Function	Dimension	Interval	Optimal value
$F_{21}(x)=-\sum_{i=1}^{5}\left[(x-a_i)-(x-a_i)^{\mathrm{T}}+c_i\right]^{-1}$	4	[0,10]	−10.153 2
$F_{14}(x)=\left[\frac{1}{500}+\sum j=1^{25}\frac{1}{j+\sum i=1^{2}(x_i-a_{ij})^6}\right]^{-1}$	2	[−65,65]	1
$F_{20}(x)=-\sum_{i=1}^{4}c_i\exp\left[-\sum_{j=1}^{6}aij(x_j-p_{ij})^2\right]$	6	[0,1]	−3.32
$F_{15}(x)=\sum_{i=1}^{11}\left[ai-\frac{x_1(bi^2+bix_2)}{bi^2+bix_3+x_4}\right]^2$	4	[−5,5]	0.000 30

To accurately evaluate the performance of each algorithm, the population number is set to be 50. The optimal solutions of the four functions at 30, 50 and 100 iterations are shown in Table 3.

Table 3 Results of four functions at 30, 50 and 100 iterations

Test function	Genetic algorithm	30 iterations	50 iterations	100 iterations
F_{21}	CSA	**−10.153 1**	−10.151 9	−10.153 2
	SSA	−5.055 0	−10.152 6	−10.153 2
	AVOA	−10.151 3	−10.153 1	−10.153 2
	TSSA	−10.007 1	−10.153 2	−10.153 2
	LOGISTIC	−10.134 4	−10.131 2	−10.153 2
	TLBO	−9.881 5	−10.152 7	−10.153 2
	TAVOA	−10.152 3	**−10.153 2**	**−10.153 2**
F_{14}	CSA	1.992	0.998 1	0.998 0
	SSA	0.899	0.998 0	0.998 0
	AVOA	1.992	0.998 3	5.928 8
	TSSA	2.982 1	1.928 8	0.998 0
	LOGISTIC	1.670 5	0.998 1	0.670 5
	TLBO	1.485 8	0.998 0	0.998 0
	TAVOA	**0.998 0**	**0.998 3**	**0.998 4**
F_{20}	CSA	−3.314 7	−3.321 6	−3.322
	SSA	−3.241 8	−3.305 9	−3.320 1
	AVOA	−2.938 2	−3.322 0	−3.322 0
	TSSA	−3.248 4	−3.318 4	−3.319 5
	LOGISTIC	−2.982 7	−2.965 5	−3.014 7
	TLBO	−3.302 9	−3.322 0	−3.322 0
	TAVOA	**−3.321 7**	**−3.321 6**	**−3.320 1**
F_{15}	CSA	0.001 295	0.000 328	0.000 347
	SSA	0.000 308	0.000 336	0.000 313
	AVOA	**0.000 321**	0.000 320	0.000 319
	TSSA	0.000 316	0.000 311	0.000 325
	LOGISTIC	0.000 566	0.000 496	0.000 347
	TLBO	0.000 751	0.000 741	0.000 783
	TAVOA	0.000 329	**0.000 324**	**0.000 313**

After replacing the random number of the African condor algorithm with Tent chaotic mapping when initializing the population, the algorithm's operation performance on the above low-dimensional functions is improved to a large extent.

It can be seen from Table 3 that when function 14 and function 20 are iterated 30 times, 50 times and 100 times, respectively, the optimization results of TAVOA algorithm are closer to the optimal value than that of other algorithms, and the optimal solutions of function 21 and function 15 are more accurate after 100 iterations.

4.1.2 High-dimensional single objective functions

To verify the performance of the improved African condor algorithm on high-dimensional single objective test functions, four high-dimensional test functions were selected for experiments. Table 4 presents the specific function expression, dimension, initial search space and optimal solution of the objective functions of four high-dimensional test functions.

The graphs of objective functions and the convergence curves of functions at iteration 100 times are shown in Figs. 3 — 6. The convergence speed and global search ability of the AVOA with excellent strategy are improved to a large extent after the random number with an interval of [0, 1] is replaced by the chaotic sequence generated by Tent chaotic mapping function. According to the convergence curves shown in Figs. 3 — 6, in the high-dimensional single-objective benchmark function 8, TAVOA obtains the optimal solution of the closest function compared with other functions after 100 iterations.

Table 4 High-dimensional single objective functions

Function	Dimension	Interval	Optimal value
$F_8(x)=\sum_{i=1}^{n}-x_i\sin\sqrt{\lvert x_i\rvert}$	30	[−500, 500]	0
$F_9(x)=\sum_{i=1}^{n}\left[x_i^2-10\cos(2\pi x_i+10)\right]$	30	[−5.12, 5.12]	0
$F_{11}(x)=\frac{1}{4\,000}\sum_{i=1}^{n}x_i^2-\prod_{i-1}^{n}\cos\frac{x_i}{\sqrt{i}}+1$	30	[−500, 500]	0
$F_{13}(x)=\frac{\pi}{n}\left\{10\sin(\pi y_1)+\sum_{i=1}^{n-1}(y_i-1)^2\left[1+10\sin^2(\pi y_{i+1})\right]+(y_n-1)^2\right\}+\sum_{i=1}^{n}u(x_i,10,100,4)$	30	[−5, 0]	0

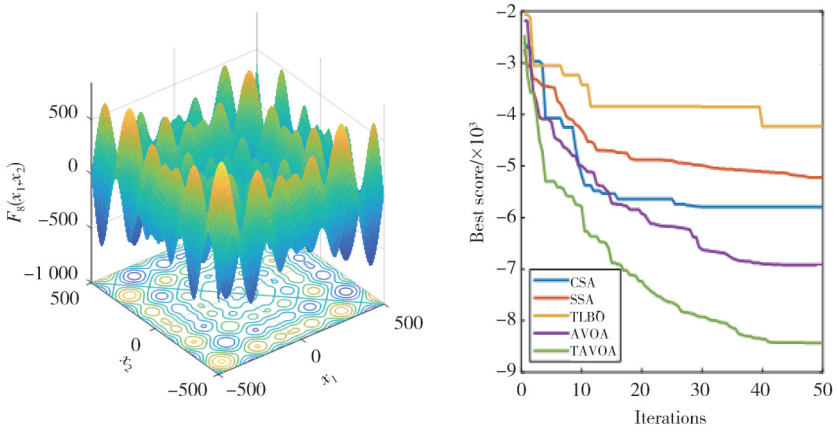

(a) Search space (b) Objective space

Fig. 3 Comparison of convergence curves of algorithms on $F_8(x)$

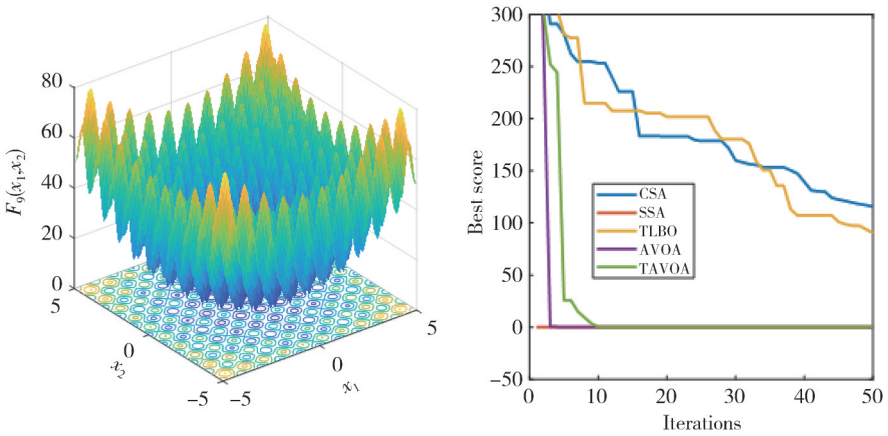

(a) Search space (b) Objective space

Fig. 4 Comparison of convergence curves of algorithms on $F_9(x)$

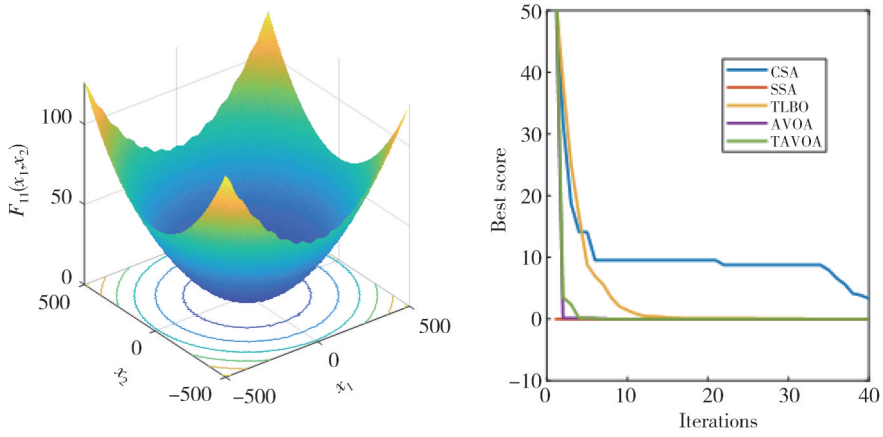

(a) Search space (b) Objective space

Fig. 5 Comparison of convergence curves of algorithms on $F_{11}(x)$

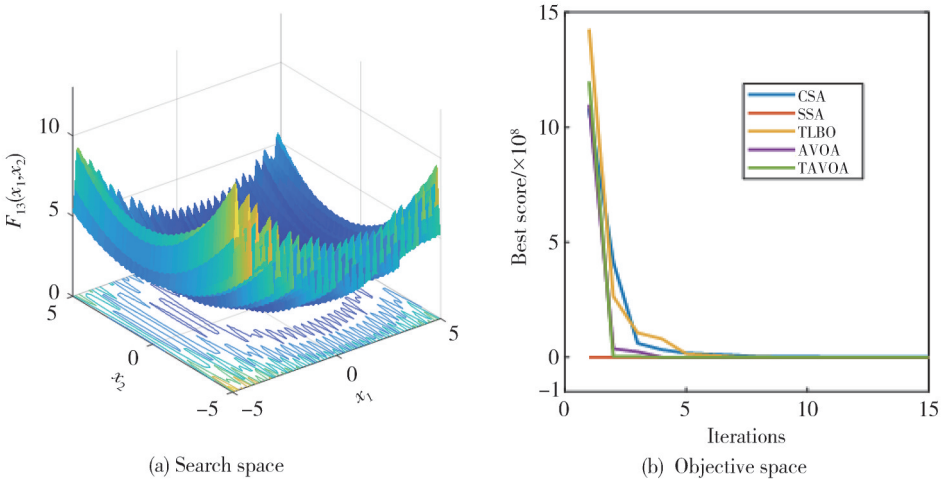

(a) Search space (b) Objective space

Fig. 6 Comparison of convergence curves of algorithms on $F_{13}(x)$

When the number of iterations of function 9 reaches 80 times, CSA and TLBO still cannot find the optimal solution of the function. With the increase of iteration times, the optimal solutions found by other algorithms are close to the optimal value of the test function 0, but TAVOA algorithm has the fastest convergence speed. In the iteration process of function 11 and function 12, both SSA algorithm and LOGISTIC algorithm fall into local optimum, while TAVOA algorithm converges faster than TLBO algorithm. Therefore, compared with the single algorithm, the improved optimization algorithm has faster convergence speed and higher accuracy, and has a certain development ability in high-dimensional single objective test function.

4.1.3 High-dimensional multi-objective function

To verify the performance of improved AVOA on high-

dimensional multi-objective test functions, four high-dimensional test functions were selected for experiments. The four test functions have different Pareto optimal solution frontiers with different shapes, which can be used to investigate the performance of the algorithm when solving different optimal solution sets. Table 5 shows the number of objective functions (f_1, f_2, and f_3) and the trends of four high-dimensional test functions. The number of iterations of each function is 100, the mesh number of each layer is 20, and the population number is 200.

Table 5 Low-dimensional objective functions

Function	Number of objective functions	Trend description
ZDT1	2 (f_1, f_2)	Convex, continuous
ZDT3	2 (f_1, f_2)	Concave, discontinuous
Viennet3	3 (f_1, f_2, f_3)	Continuous, multimodal
Kursawe	2 (f_1, f_2)	Discontinuous, multimodal

Table 6 Comparison of running times

Function	Running time/min			
	MOSSA	MNCSA	MOAVOA	TMOAVAO
ZDT1	15.734	15.157	15.964	**14.839**
ZDT3	14.793	14.074	14.453	**13.236**
Viennet3	17.682	17.089	18.107	**17.447**
Kursawe	11.897	11.786	13.878	**11.761**

In this experiment, MOSSA, MNCSA, MOAVOA, and TMOAVAO algorithms were compared in the average running time, and the running times were 20. Table 6 presents the comparison of experimental results. It can be seen from that after combining the excellent strategy of improved African condor optimization algorithm with the multi-objective optimization algorithm with elite strategy, the average running time of TMOAVOA algorithm is the shortest after 20 iterations.

The non-inferior solution frontiers of four algorithms on four test funtions are shown in Figs. 7—10. It can be seen that using the data generated by Tent chaotic mapping as the initial position of vulture population can improve the convergence speed of the algorithm.

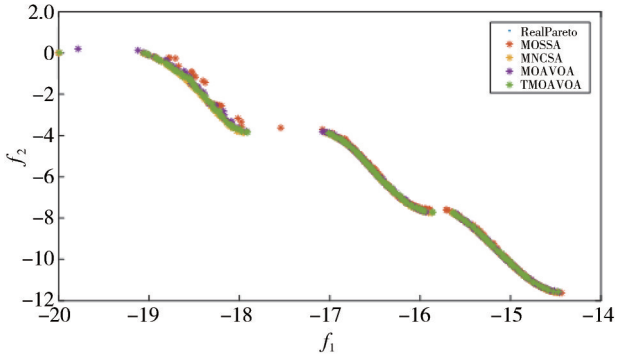

Fig. 7 Function Kursawe fitting comparison diagram

In addition, compared with other multi-objective optimization algorithms, TMOAVOA algorithm can quickly find Pareto solutions on the four multi-objective data sets, and the solution speed is fast.

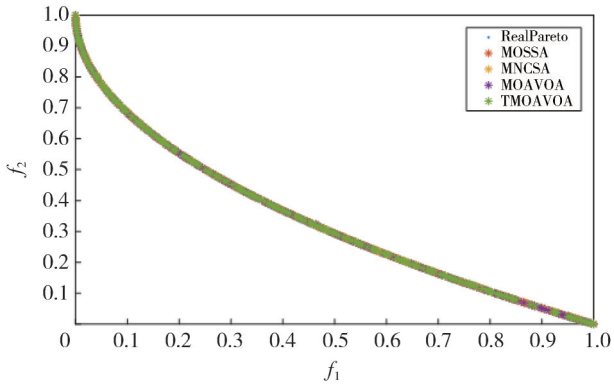

Fig. 8 Function ZDT1 fitting comparison diagram

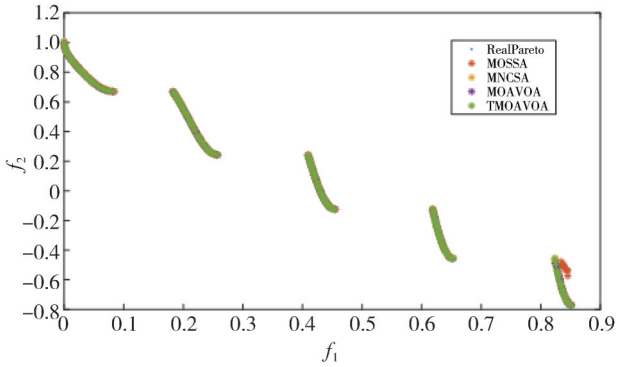

Fig. 9 Function ZDT3 fitting comparison diagram

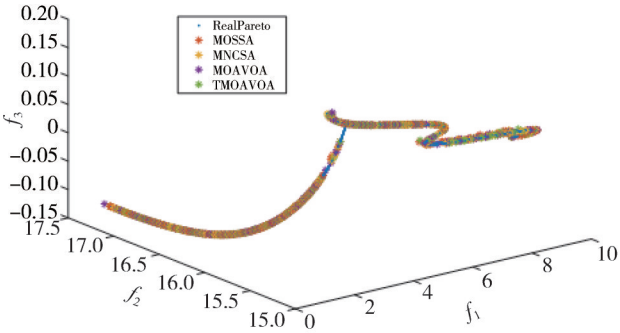

Fig. 10 Function Viennet3 fitting comparison diagram

4.2 Application of VMD

In actual wind power prediction, due to strong volatility and randomness of wind power data samples, if the original sequence is directly input into the prediction model as a training set, the upper and lower limits of the sample data may result in "false components" and "endpoint effect" in the model prediction. VMD is a kind of time-frequency signal decomposition method for unsteady signal processing and analysis. The original wind power sequence has strong fluctuation and nonlinear characteristics, so VMD method can be used

for noise reduction. The original wind power sequence can extract low-frequency signals that more accurately describe the changes of wind power. The original sequence diagram is shown in Fig.11.

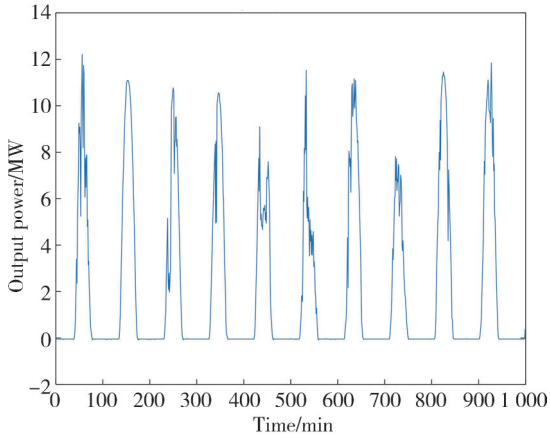

Fig. 11 Original sequence diagram of wind power

In this study, the original wind power was decomposed into five layers. During the decomposition process, the data adaptively matched with the optimal center frequency and broadband of each sequence. Four eigenmode components and one residual component were obtained, and high frequency and low frequency signals of wind power were obtained by decomposition. Here, 6 502 samples data were selected in spring. It can be seen from Fig.12 that IMF_4 and Res components fluctuate violently, with obvious nonlinear characteristics and complex wave forms.

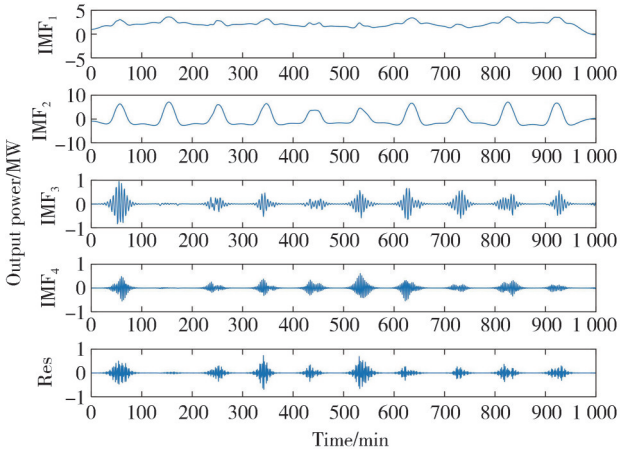

Fig. 12 Wind power decomposition

The variation of IMF_3 component is relatively gentle, and the degree of complexity decreases. IMF_1 and IMF_2 show significant regularity, and the sequence variation trends are simple and easy to analyze.

Due to the auto-correlation of time series, the prediction lag phenomenon will occur when the prediction of non-stationary time series is made directly, that is, the predicted value of the current time is almost equal to the predicted value of the last time, and there is a certain lag between the predicted value and the real value, especially in the position where the data rise or fall rapidly, as shown in Fig.13.

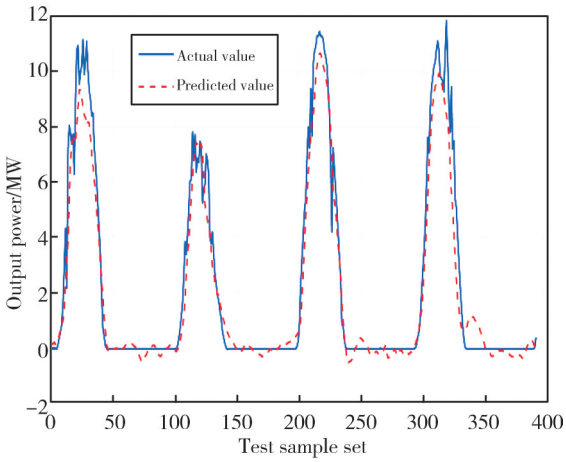

Fig. 13 LSSVM wind power fitting diagram

Here, the VMD method was used to reduce the complexity of the original sequence and decompose the original sequence into several relatively stable sub-sequences to solve the prediction lag problem. VMD-LSSVM model can effectively solve the prediction lag problem and improve the prediction accuracy of the model. The fitting diagram after VMD is shown in Fig.14.

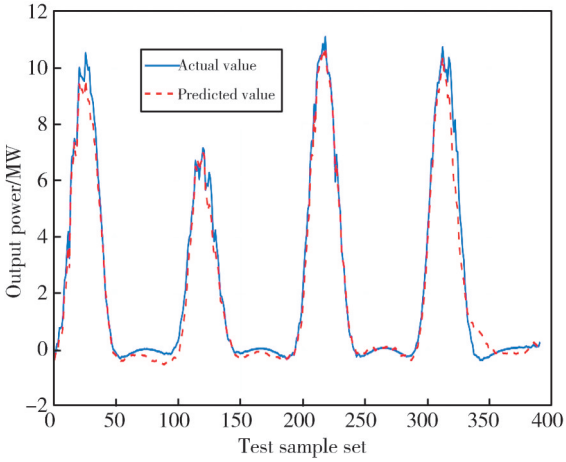

Fig. 14 VMD-LSSVM wind power fitting diagram

4.3 Evaluation indicators

In this study, the historical power and wind speed data of a real wind power station in 2019 in four seasons were used. The samples data were the average power data set every 15 min, and the number of samples in each season was 6 502. Wind speed, wind direction, ambient temperature, relative humidity, atmospheric pressure, scattered radiation area, direct radiation area, theoretical power of photometry, and output power of the whole station were taken as input variables, and wind power value was taken as output index. The first 3 902 (top 60%) samples of the

whole data set were selected as the training set, and the last 2 600 (bottom 40%) samples data were selected as the test set. Zero-value interpolation method was used for missing values in the data set. To eliminate the dimensional influence between different evaluation indexes, z-score standardization method was used to normalize the data, so as to compare the prediction results of the model. It is defined as

$$x_k^* = \frac{x - \mu}{\sigma}, \tag{22}$$

where μ is the mean of all samples data, and σ is the standard deviation of all samples data.

To verify the performance of the model from the perspective of horizontal prediction accuracy and vertical prediction accuracy, root mean square error (RMSE), mean absolute error (MAE), mean absolute percentage error (MAPE) and direction statistics (DS) are selected as the performance evaluation indexes of the prediction model. Among them, DS is used to judge whether the predicted results of the model change in the same direction as the real value, which is commonly used in nonlinear data with large volatility. The evaluation index formulae are expressed as

$$\sigma_{\mathrm{RMSE}} = \sqrt{\frac{1}{n}\sum_{i=1}^{n}\left| y_i - \hat{y}_i \right|^2}, \tag{23}$$

$$\sigma_{\mathrm{MAE}} = \frac{1}{n}\sum_{i=1}^{n}\left| y_i - \hat{y}_i \right|^2, \tag{24}$$

$$\sigma_{\mathrm{MAPE}} = \frac{1}{n}\sum_{i=1}^{n}\left| \frac{y_i - \hat{y}_i}{y_i} \right| \times 100\%, \tag{25}$$

$$\sigma_{\mathrm{DS}} = \frac{1}{n}\sum_{i=1}^{n} w_i, \tag{26}$$

where $g(x) = (y_i - y_{i-1})(y_i^* - y_{i-1}) > 0$ is constraint. If it is met, w_i is 1; otherwise, it is 0.

4.4 Discussion

In this section, we select RBF neural network, BP neural network, LSSVM single model, single-objective optimization SSA-LSTM, single-objective optimization CSA-LSSVM (CLSSVM) model, single-objective optimization AVOA-LSSVM (ALSSVM) model, single-objective optimization TLBO-LSSVM (TBLSSVM) model, single-objective optimization LSSA-LSSVM (LSLSSVM) model based on Logistic chaotic mapping improved SSA algorithm, single-objective optimization model TALSSVM based on Tent chaotic mapping improved AVOA algorithm, VMD-LSSVM (VLSSVM) model, VMD-SSA-LSSVM (VSALSSVM) model, Multi-objective SSA algorithm optimization LSSVM (MOSLSSVM) model, NSGA-based multi-objective optimization LSSVM (MNCLSSVM) model, and MOAVOA-VMD-LSSVM (MOALSSVM), and the proposed hybrid TMOAVOA-VMD-LSSVM (TMOALSSVM) model to compare the prediction results with the actual results on the wind power data set, and the prediction effects of different prediction models are reflected by fitting curves. In the experiment, the learning rate of both RBF neural network and BP neural network was set to be 0.01, the number of hidden layers was 3, the number of training iterations was 1 000, and the number of hidden layers was 128. The activation function of BP neural network was tanh function, and the activation function of RBF neural network was Gaussian function. The GAM value of LSSVM model was set to be 10, and the SIG2 value was set to be 1 000. The population number of the single objective optimization prediction intelligent optimization algorithm was 50, the dimension of optimization parameters was 2, the population number of the multi-objective optimization intelligent optimization algorithm was 200, the number of iterations was 100, the crossover probability of MOCSA algorithm and MOAVOA algorithm was 0.9, the mutation probability was 0.03, and the ratio of producers in the SSA algorithm was 0.2. Table7 presents the performance of different evaluation indexes in different models in four seasons.

In a single model, the three error analysis values of LSSVM model on the wind power data set are all small, and the accuracy of prediction results is high. Thus, LSSVM is the optimal benchmark model with better stability and adaptability. TALSSVM model and TMOALSSVM model are the optimal models in single objective models and mult-objective models, respectively. After combining the intelligent optimization algorithm withsingle objective LSSVM model optimization, the errors of each model on the data set are reduced to a certain extent. Among them, the improved TALSSVM model based on Tent chaotic mapping has the lowest evaluation indexes in three seasons. Compared with logistic chaotic mapping, Tent chaotic mapping can retain the diversity of population, accelerate the convergence speed of the algorithm, and improve the global search ability, thus improving the prediction accuracy of the model. Compared with the single model, the prediction model with VMD method reduces three error values to different degrees, which means that the VMD method is an effective and feasible method for the prediction of some non-stationary time series.

Table 7 Comparison of prediction results

Model	Spring			Summer			Autumn			Winter		
	RMSE	MAE	MAPE	RMSE	MAE	MAPE	RMSE	MAE	MAPE	RMSE	MAE	MAPE
BP[8]	0.856 1	0.527 1	0.147 7	1.692 3	1.509 1	1.422 7	0.570 2	0.490 6	0.369 2	1.763 2	1.485 9	0.336 6
RBF[9]	0.841 3	0.527 6	0.164 2	1.248 6	0.925 6	0.417 2	0.578 3	0.503 9	0.379 9	1.011 6	0.857 5	0.398 9
LSSVM[10]	0.791 7	0.487 1	0.130 8	1.083 7	1.065 2	1.028 5	0.509 6	0.418 7	0.363 8	1.760 6	1.482 5	0.335 9
SLSSVM[13]	0.725 9	0.449 6	0.093 2	1.244 7	1.062 3	1.027 2	0.675 1	0.419 8	0.364 1	0.692 3	0.509 1	0.422 7
CLSSVM[23]	0.624 7	0.408 6	0.100 9	1.251 6	0.972 4	0.416 9	0.676 9	0.571 5	0.418 3	0.574 2	0.433 0	0.381 5
ALSSVM	0.645 9	0.441 0	0.104 3	1.083 4	0.972 1	0.411 4	0.509 1	0.569 0	0.411 3	0.574 2	0.433 1	0.381 5
TBLSSVM[14]	0.587 2	0.450 2	0.103 9	1.167 8	0.985 4	0.537 6	0.623 1	0.589 1	0.392 6	0.623 3	0.415 3	0.392 1
LSLSSVM[15]	0.648 9	0.431 2	0.104 5	1.130 9	1.500 4	0.390 6	0.049 4	0.040 1	0.029 7	0.153 7	0.142 5	0.134 2
TALSSVM	0.622 1	0.438 5	0.092 6	1.053 1	0.980 4	0.223 2	0.049 1	0.038 7	0.027 9	0.122 3	0.098 9	0.024 9
VLSSVM	0.625 2	0.359 8	0.083 9	0.088 4	0.078 6	0.029 9	0.043 5	0.032 8	0.023 9	0.113 4	0.090 6	0.023 2
VALSSVM	0.168 3	0.132 2	0.031 6	0.077 4	**0.030 1**	0.021 3	0.043 1	0.029 8	0.022 3	0.056 4	0.050 4	**0.020 6**
MOSLSSVM	0.100 5	0.154 2	0.015 1	0.074 0	0.077 1	0.020 9	0.593 1	0.509 7	0.423 2	0.062 8	0.040 7	0.037 0
MNCLSSVM[24]	0.121 2	0.127 3	0.026 8	0.079 1	0.038 7	0.027 9	0.692 3	0.509 1	0.422 7	0.067 2	0.049 5	0.032 2
MOALSSVM	0.113 3	0.126 2	0.021 0	0.089 4	0.060 1	**0.019 7**	0.043 2	0.032 1	0.021 3	0.058 9	0.046 3	0.027 2
TMOALSSVM	**0.105 9**	**0.114 3**	**0.014 8**	**0.067 3**	**0.030 1**	0.025 4	**0.041 3**	**0.030 5**	**0.020 4**	**0.053 1**	**0.042 9**	0.023 8

From the perspective of transverse accuracy MAE, the average MAE of single objective AVOA (VALSSVM) is 0.069 9 in four seasons, the MAE of MOSLSSVM is 0.195 4 in four seasons, and the MAE average of MOAVLSSVM is 0.066 2 in four seasons. AVOA algorithm has better global search ability due to its excellent sharing strategy. The comparison of the average error values of transverse and longitudinal prediction of all models is shown in Fig.15.

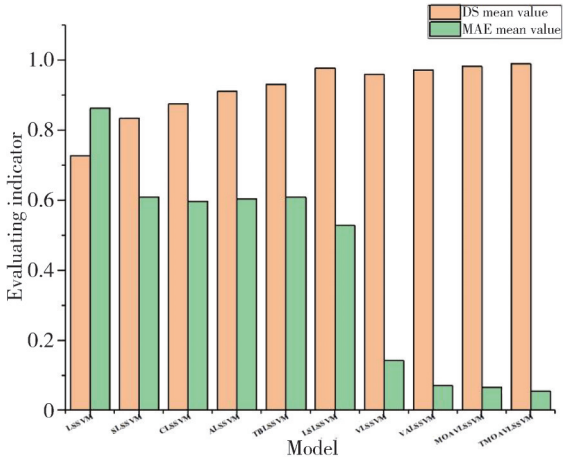

Fig. 15 Comparison of longitudinal and horizontal errors

The proposed MOAVOA considers the directional accuracy, horizontal prediction error, and vertical prediction error. LSSVM is used as the benchmark model for comparison, as shown in Table 7. In summer, the MAE value of transverse prediction accuracy of VALSSVM model and TMOALSSVM model are 0.030 1. In Fig.15, the average DS value of longitudinal prediction accuracy of TMOALSSVM is 0.990 2 increased by 0.016 4 compared to the average DS value of VALSSVM model, indicating that the multi-objective optimization algorithm can better find the optimal Pareto solution set of prediction accuracy in different directions under the current constraints. The fitting diagram of prediction results of the models is shown in Fig.16. It also can be seen that compared with other models, the trend of TMOALSSVM model is closer to the change trend of the real value, and the prediction accuracy is higher.

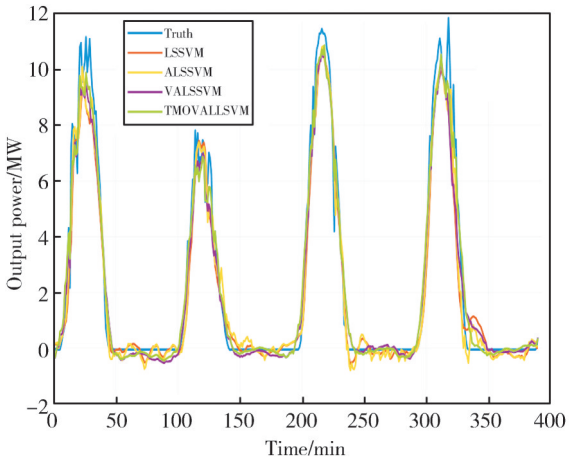

Fig. 16 Fitting diagram of prediction results

5 Conclusions

Considering to further improve the accuracy of wind power prediction in different directions considering nonlinear non-stationary sequences with strong fluctuation, a hybrid prediction model based on VMD and MOAVOA was proposed. Firstly, the non-stationary original wind power time sequence was decomposed and otherinto five intrinsic mode components by VMD method, which solves the problems that there exists a prediction lag phenominon by using a single model, thus reduceing the complexity of the original data and non-stationary influence on forecast results. Furthermore, to improve the prediction accuracy of the model, the improved TMOALSSVM based on Tent chaotic mapping and non-dominated

sorting with elite strategy was used to predict the decomposed components. Finally, the final prediction result was obtained by integrating and summing the predicted components. The proposed multi-object optimization model and other models were experimentally compared. The results show that the proposed model can more quickly and accurately find the Pareto optimal solution in the horizontal and vertical directions, so as to improve the prediction accuracy of the model in different directions as well as the overall prediction performance.

In the following research, the dynamic environmental and economic dispatching of the power system will be further considered, power generation cost and pollution gas emission will be set as objective functions, and more constraints will be added, so as to improve the prediction accuracy of wind power and bring economic and environmental benefits to the power system.

Acknowledgement

This work was supported by National Natural Science Foundation of China (Nos. 61662042, 62062049); Science and Technology Plan of Gansu Province (Nos.21JR7RA288, 21JR7RE174).

Declaration of conflicting interests

The authors have no conflict of interests related to this publication.

References

[1] LI Q S, ZHANG K. The path for green development and utilization of energy in China. Chinese Journal of Engineering Science, 2021, 23(1): 101-111.

[2] YUN Y Y, DONG H Y, CHEN Z, et al. Multi-objective optimization scheduling for new energy power system considering energy storage participation. Journal of Measurement Science and Instrumentation, 2020, 11(4): 365-372.

[3] ZHANG Q, TANG Z H, WANG G, et al. Ultra-short-term wind power prediction model based on long and short term memory network. Acta Energiae Solaris Sinica, 2021,42(10): 275-281.

[4] YE L, ZHAO Y N, ZENG C, et al. Short-term wind power prediction based on spatial model. Renewable Energy, 2017, 101: 1067-1074.

[5] CAO J B, ZHOU R J, DENG X H, et al. Wind power forecast considering differential times of optimal ARIMA model. Proceedings of the CSU-EPSA, 2019, 31(1): 105-111.

[6] ZHANG L D, LI J Y, WU Y, et al. ARIMA model forecast for wind power time series with different temporal resolutions. Electric power, 2016, 49(6): 176-180.

[7] CUI Y, CHEN Z H, XU P H. Short-term power prediction for wind farm and solar plant clusters based on machine learning method. Electric Power, 2020, 53(3): 1-7.

[8] HE T Y, TIAN X C, LI S N, et al. Improved BP neural network based on Artificial Bee Colony algorithm for wind power prediction. Journal of Electric Power Science and Technology, 2018, 33(4): 22-28.

[9] WANG J X, DENG B, WANG J. Short-term wind power prediction based on empirical mode decomposition and RBF neural network. Proceedings of the CSU-EPSA, 2020, 32(11): 109-115.

[10] LIU C, LANG J. Wind power prediction method using hybrid kernel LSSVM with batch feature. Acta Automatica Sinica, 2020, 46(6): 1264-1273.

[11] SUN W, GAO Q. Short-term wind speed prediction based on linear-nonlinear decomposition of variational mode decomposition combination optimization model. Journal of Energies, 2019, 12(12): 2322.

[12] ZHAO Z, ZHOU Z Y. NAN H G. Research on multi-step interval forecasting of CNN-BiLSTM ultra-short-term wind power based on VMD. Journal of North China Electric Power University (Natural Science Edition), 2022, 49(4): 91-97.

[13] WANG R, CHEN Z K, LU J. Short-term prediction of wind power based on VMD and IBA LSSVM. Journal of Hohai University (Natural Sciences), 2021, 49(6): 575-582.

[14] WEI P F, FAN X C, SHI R J, et al. Short-term photovoltaic power generation forecast based on improved sparrow search algorithm optimized support vector machine. Thermal Power Generation, 2021, 50(12): 74-79.

[15] CHENG Y L, WANG Z J, LIU S M, et al. Short-term prediction of wind power based on improved TLBO optimization LSSVM. Electrical Measurement & Instrumentation, 2019, 56(13): 81-85.

[16] TONG W G, GUO C Y, ZHAO R Y. Prediction model of slurry density in recycling tank based on LSSVM optimized by improved sparrow algorithm. Electronic Measurement Technology, 2022, 45(1): 70-76.

[17] HUANG J Y. Research on sparrow search algorithm based on fusion of T distribution and Tent chaos mapping2. Lanzhou: Lanzhou University, 2021.

[18] LIU Y F, DONG H Y, WANG N B, et al. An optimal strategy for coordinating and dispatching"source-load"in power system based on multiple time scales. Journal of Measurement Science and Instrumentation, 2018, 9(4): 388-396.

[19] YU X Y, SHEN Y X, CHEN J, et al. A multi-objective prediction method for short-term microgrid load considering interval probability. Acta Electronica Sinica, 2017, 45(4): 930-936.

[20] ABDOLLAHZADEH B, GHAREHCHOPOGH F S, MIRJALILI S. African vultures optimization algorithm: A new nature-inspired metaheuristic algorithm for global optimization problems. Computers & Industrial

Engineering, 2021, 158: 107408.
[21] FAN J H, LI Y, WANG T. An improved African vultures optimization algorithm based on tent chaotic mapping and time-varying mechanism. PLoS One, 2021, 16(11): e0260725.
[22] BRAIK M S. Chameleon swarm algorithm: A bio-inspired optimizer for solving engineering design problems. Expert Systems with Applications, 2021, 174: 114685.
[23] ZHANG M Q, WANG L, CUI Z H, et al. Fast non-dominated sorting genetic algorithm Ⅱ based on hybrid strategy. Journal of Zhengzhou University (Engineering Science), 2020, 41(4): 23-27.

基于LSSVM改进AVOA的风电功率预测应用

张忠林[1*], 魏　凡[1], 闫光辉[1], 马海云[2]

1. 兰州交通大学 电子与信息工程学院, 甘肃 兰州 730070;
2. 天水师范学院 物理与信息科学学院, 甘肃 天水 741001

摘　要: 提高风电功率预测精度是减小风电对电网影响的有效手段。为此, 提出了一种改进非洲秃鹫优化算法(African vulture optimization algorithm, AVOA)构建多目标优化最小二乘支持向量机(Least squares support vector machine, LSSVM)预测模型。首先, 利用变分模态分解(Variational modal decomposition, VMD)将原始风功率时间序列有效分解为一定数量的固有模态分量(Intrinsic modal components, IMFs)。其次, 以Tent混沌映射代替种群初始化中的随机数并引入带精英策略的非支配排序及拥挤度算子改进的AVOA算法多目标优化LSSVM, 对每个分量进行预测。最后, 利用TMOALSSVM方法分别对各分量集成加和得到最终的预测结果。仿真结果表明, 基于Tent混沌映射改进的非洲秃鹫优化算法与加入带精英策略的非支配排序、拥挤度算子改进的优化算法分别为单目标和多目标预测的最优模型。其中, 本研究所构建的模型在四个季节中风功率值三个平均误差值均为最小, RMSE、MAE以及MAPE值分别为0.069 4、0.054 5与0.021 1; 四个季节中的Ds统计量平均值为0.990 2, 统计值最大。该模型将方向预测精度作为多目标优化函数, 在横向精度和纵向精度上均对四个季节的风功率值进行了有效预测, 更快更准确地找到了当前约束条件下的最优pareto解集, 由此证明了该方法在风电功率预测技术发展领域具有一定科学意义。

关键词: 非洲秃鹫优化算法; 最小二乘支持向量机; 变模态分解; 多目标预测; 风电功率

引用格式: ZHANG Zhonglin, WEI Fan, YAN Guanghui, et al. Improved AVOA based on LSSVM for wind power prediction. Journal of Measurement Science and Instrumentation, 2024, 15(3): 344-359.